KSME

Springer

Journal of Mechanical Science and Technology 34 (11) 2020

Original Article
DOI 10.1007/s12206-020-1012-8

Keywords:
· Rolling linear guides
· Interval number
· Uncertainty
· Dynamic reliability

Correspondence to:
Yan Ran
ranyan@cqu.edu.cn

Citation:
Li, J., Ran, Y., Wang, H., Huang, G., Mu, Z., Zhang, G. (2020). Dynamic performance reliability analysis of rolling linear guide under parameter uncertainty. Journal of Mechanical Science and Technology 34 (11) (2020) 4525~4536. http://doi.org/10.1007/s12206-020-1012-8

Received May 11th, 2020
Revised July 21st, 2020
Accepted August 25th, 2020

† Recommended by Editor
No-cheol Park

Dynamic performance reliability analysis of rolling linear guide under parameter uncertainty

Jian Li[1], Yan Ran[1], Hongwei Wang[1], Guangquan Huang[1], Zongyi Mu[1] and Genbao Zhang[1,2]

[1]State Key Laboratory of Mechanical Transmissions, Chongqing University, Chongqing 400044, China, [2]School of Mechanical and Electrical Engineering, Chongqing University of Arts and Sciences, Chongqing 402160, China

Abstract This paper presents a dynamic reliability analysis method of rolling linear guide considering the uncertainty of geometric parameters. A three degree of freedom (DOF) dynamic motion model of rolling linear guide that considers the complexity of the actual load is established. In order to improve the accuracy of reliability evaluation, interval model is used to express the uncertainty of geometric parameters. The reliability range of dynamic response is determined according to the accuracy grade of rolling linear guide. The interval reliability calculation method is used to analyze and calculate the horizontal and vertical dynamic reliability of rolling linear guide. Then, the comprehensive dynamic reliability of rolling linear guide is obtained. Finally, the dynamic reliability of the SHS-45R rolling linear guide is analyzed by using the reliability evaluation method described in this paper. And the validity and accuracy of the result is demonstrated by comparing with the Monte Carlo simulation.

1. Introduction

In recent years, CNC machine tool is developing towards high speed and high precision, which put forward higher requirements for machining performance and stability. The rolling linear guide has the advantages of high positioning accuracy, small friction coefficient, good accuracy retention, good maintainability and so on. It has become an important functional component of CNC machine tool [1]. Thus, it is necessary to study the dynamic characteristics of rolling linear guide to ensure the machining performance of machine tools [2, 3].

The influence of various factors on the dynamic performance of rolling linear guide has been studied, such as friction, wear and preload. Yi et al. [4] studied the influence of friction on the dynamic characteristics of linear guide by experiment and theoretical method. Zou et al. [5] established a prediction model of contact stiffness by studying the change of contact stiffness caused by friction and wear during the use of rolling linear guide. Tao et al. [6] predicted the wear and performance of rolling linear guide by establishing the displacement calculation model that caused by the wear of carriage. Li et al. [7] studied the effect of bolt joint on the dynamic characteristics of linear guide. The dynamic characteristics that influenced by the preload, rolling ball diameter and initial contact angle were studied by Kong et al. [8]. Considering the flexible of the carriage, Tong et al. [9] constructed the stiffness matrix for a five degree of freedom (DOF) model of a linear rolling guide. However, in practical project, there are inevitably uncertain factors such as material performance, geometric dimension, load and so on, resulting in the uncertainties of the machining process [10]. When the parameters are uncertain, the random reliability analysis method is usually used to evaluate the reliability, for instance, Sao et al. [11] calculated the dynamic reliability of the manipulator based on the Monte Carlo simulation (MCS) method, Li et al. [12] studied the reliability of the power tool turret under the condition of uncertain parameters through the first-order reliability method (FORM), Zhou et al. [13] established the reliability analysis model of gear system according to the saddle point approximation (SPA) method.

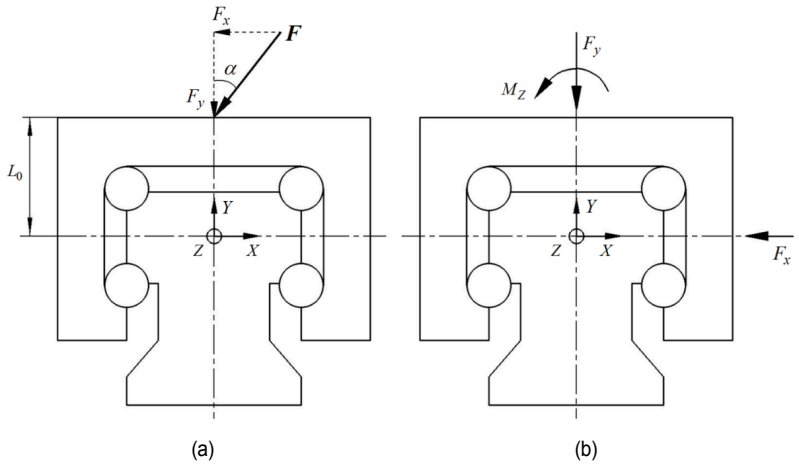

Fig. 1. The load analysis of the rolling linear guide.

However, the above analysis methods have the disadvantages of large amount of calculation or large error of results, which limits its application in the dynamic reliability analysis of rolling linear guide. In order to overcome the shortcomings of the traditional random reliability analysis method, Wang et al. [14] used the normal distribution to represent the uncertainty of the geometric parameters, and the statistical moment of dynamic error was calculated by using random perturbation method to evaluate the dynamic reliability of rolling linear guide.

When using the random reliability analysis method, it is necessary to assume that the geometric parameters obey the determined probability distribution. However, in practical engineering problems, there are some problems, such as the small number of test samples and difficulties in data acquisition [15, 16]. Due to the lack of data, it is difficult to obtain the accurate probability distribution of parameters [17, 18]. When the probability distribution of geometric parameters is assumed, even if there is a slight change from the real value, it may cause large calculation error [19, 20]. Although the probability distribution of the uncertain parameters cannot be defined accurately, the upper and lower bounds of it can be easily determined, so the interval model can be used to deal with the uncertainty of parameters [20-22]. Interval analysis method only needs to know the upper and lower bounds of the uncertain parameters without knowing their specific distribution. It can retain the original information of uncertain parameters and make the analysis results more in line with the practicalities, so it has been widely used in reliability analysis and optimization [23-25].

In addition, in the dynamic reliability analysis, only the effect of vertical load is analyzed. Nevertheless, the loads of rolling linear guide in the actual work process are complex and diverse [26]. Under complex loads, the dynamic reliability analysis of rolling linear guide includes the vertical dynamic reliability and the horizontal dynamic reliability. Therefore, it is necessary to consider the actual load of rolling linear guide and establish a suitable dynamic motion model to make the analysis results more in line with the engineering practice.

The purpose of this paper is to evaluate the dynamic reliability of rolling linear guide accurately. In order to improve the accuracy of the evaluation results, the interval model is used to express the uncertainty of the geometric parameters of rolling linear guide. Considering the complex load in the actual working process, the dynamic characteristics of rolling linear guide are analyzed by using two-DOF dynamic motion model and three-DOF dynamic motion model respectively. And the effecting mechanism of complex loads on the dynamic characteristics of rolling linear guide is explained by comparing the results. Then, the three-DOF dynamic motion model is used to analyze the reliability of rolling linear guide. The interval values of vertical and horizontal displacement dynamic responses of rolling linear guide are obtained. Thus, the interval reliability calculation method is introduced to evaluate the vertical and horizontal dynamic reliability of rolling linear guide. Finally, the comprehensive dynamic reliability is obtained.

The rest of the paper is organized as follows: in the next section, based on Hertz contact theory, considering the complexity of the actual load and analyzing the load and contact deformation of rolling linear guide, the dynamic motion model is established. The reliability calculation method based on interval model is introduced in Sec. 3, and the dynamic reliability calculation model is established. In Sec. 4, taking the SHS-45R for example, the analysis results of two-DOF dynamic motion model and three-DOF dynamic motion model are compared, and the effect of complex loads is explained. The dynamic reliability of the rolling linear guide is analyzed by the proposed method, and the validity and accuracy of the method are verified. Finally, some brief conclusions are obtained in Sec. 5, which are of guiding significance to the design and application of rolling linear guide.

2. Dynamic analysis and modeling of rolling linear guide

2.1 The load analysis and modeling

As shown in Fig. 1, in the actual operation process, rolling linear guide is affected by complex working load $\boldsymbol{F}$. The load

acts on the center of the carriage and the angle between the load and the vertical direction is α. Considering the actual working condition, the load is expressed by the simple harmonic excitation force [27, 28]. In order to facilitate the dynamic analysis and modeling of rolling linear guide, the Cartesian coordinate system O-XYZ is established. As shown in Fig. 1(b), the working load that acting on carriage include: vertical load F_y, horizontal force F_x and moment M_Z. And the calculation expressions of the loads F_x, F_y and M_Z are:

$$\begin{cases} F_x = \boldsymbol{F}\sin\alpha \\ F_y = \boldsymbol{F}\cos\alpha \\ M_Z = F_x L_0 = (\boldsymbol{F}\sin\alpha) L_0 . \end{cases} \tag{1}$$

2.2 Positioning error analysis of rolling linear guide

The dimensional tolerance and walking parallelism tolerance are the main precision tolerances of rolling linear guide [14]. The dimensional tolerance can be reduced by improving the installation precision of rolling linear guide [29]. As shown in Fig. 2, in the actual working process, the vertical displacement V and horizontal displacement H are produced due to the effect of the working load. However, since the uncertainty of geometric parameters, the values of V and H fluctuate at every moment, which is not equal to the ideal value. Therefore, the parallelism error in the moving process of rolling linear guide is produced.

2.3 Load and contact deformation of rolling linear guide

The structure of rolling linear guide is illustrated in Fig. 3, mainly including three parts: carriage, rolling balls and rail. Due to the effect of load F_x, F_y and M_Z, the carriage produces vertical displacement V, horizontal displacement H and deflection angle θ. Where, $i\,(i=1,2,3,4)$ is the raceway number, $Q_i\,(i=1,2,3,4)$ indicates the contact force of the rolling balls. The Hertz contact theory is used to analyze contact effect between the rolling ball and the groove. And the contact model between the rolling balls and groove is shown in Fig. 4. O_{ci} is initial groove curvature centers of carriage, O_{ri} is the initial groove curvature centers of rail. R_c is the radius of curvature of carriage, R_r is the radius of curvature of rail. β_0 is initial contact angle.

The initial contact deformation of rolling balls is δ_0, and it is caused by the preload of linear guide rail. The initial distance s_0 between O_{ci} and O_{ri} can be written as:

$$s_0 = R_c + R_r - d + \delta_0 \tag{2}$$

where d indicates the initial distance between the rail groove and the carrier groove, d_0 represents the ball diameter without deformation. The deformation of the ball δ_0 is:

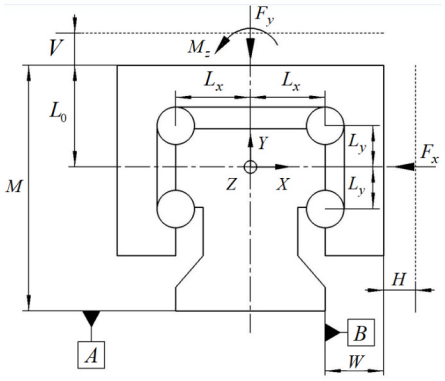

Fig. 2. Precision tolerances of rolling linear guide.

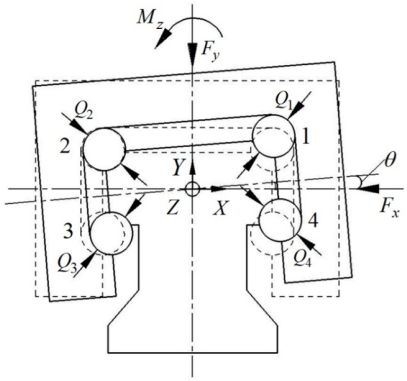

Fig. 3. Simplified model of rolling linear guide.

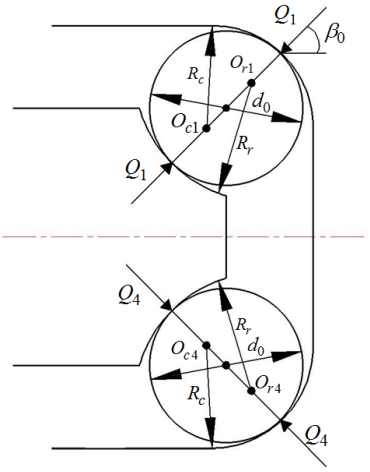

Fig. 4. Initial deformation of rolling linear guide without load.

$$\delta_0 = d_0 - d . \tag{3}$$

According to the Hertz contact theory, the contact force between rolling balls and groove can be expressed as [26, 30]:

$$Q_i = \frac{(\delta_i)^{3/2}}{\mu^{3/2}\left[\frac{9}{4}\left(\left(\frac{1-\boldsymbol{v}_1^2}{\boldsymbol{E}_1}+\frac{1-\boldsymbol{v}_2^2}{\boldsymbol{E}_2}\right)^2(\sum\rho)\right)\right]^{3/2}} \tag{4}$$

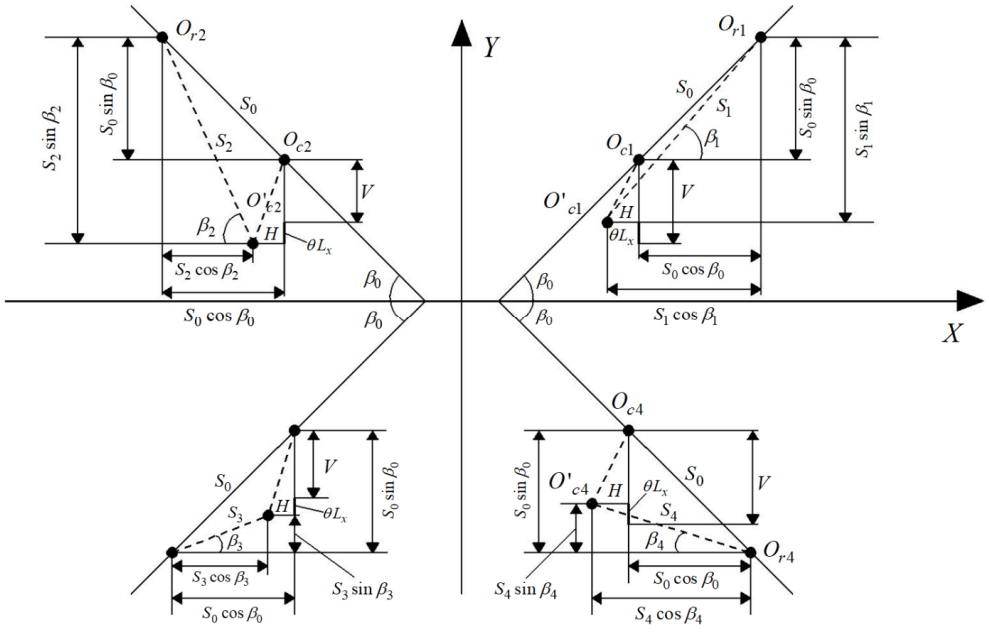

Fig. 5. Geometrical relationship of displacement and deformation.

where δ_i indicates the elastic deformation of rolling ball; $\boldsymbol{\nu}_1, \boldsymbol{\nu}_2$ are elastic moduli, $\boldsymbol{E}_1, \boldsymbol{E}_2$ are Poisson ratios. μ is the Hertz coefficient related to the stiffness, $\sum\rho$ is the main curvature of rolling balls and groove. μ and $\sum\rho$ can be obtained by using the Hertz contact theory [31]. The Eq. (4) is simplified as:

$$Q_i = \xi\delta_i^{3/2} . \tag{5}$$

ξ is the contact coefficient, and it describes the relationship between contact load Q_i and the elastic deformation of rolling balls.

$$\xi = \mu^{3/2}\left[\frac{9}{4}\left(\left(\frac{1-\boldsymbol{\nu}_1^2}{\boldsymbol{E}_1}+\frac{1-\boldsymbol{\nu}_2^2}{\boldsymbol{E}_2}\right)^2\left(\sum\rho\right)\right)\right]^{-(1/2)} . \tag{6}$$

Under the load F_x, F_y and M_Z, the deformation of rolling balls moves from δ_0 to $\delta_i (i=1,2,3,4)$. In order to simplify the relationship between the deformation and the contact force, it is assumed that the elastic deformation is mainly concentrated on the rolling balls and the rail is fixed [14, 26]. The relationship between the displacement of carriage and the deformation of rolling balls are illustrated in Fig. 5, the initial curvature centers O_{ci} and O_{ri} move to the new position O'_{ci} and O'_{ri}.

Through analysis and calculation, the elastic deformation of each row of rolling balls are shown as follows:

$$\begin{aligned}\delta_1 &= S_1 - S_0 + \delta_0 \\ &= \sqrt{\left(S_0\sin\beta_0 + V - \theta L_x\right)^2 + \left(S_0\cos\beta_0 + H\right)^2} - S_0 + \delta_0\end{aligned} \tag{7}$$

$$\begin{aligned}\delta_2 &= S_2 - S_0 + \delta_0 \\ &= \sqrt{\left(S_0\sin\beta_0 + V + \theta L_x\right)^2 + \left(S_0\cos\beta_0 - H\right)^2} - S_0 + \delta_0\end{aligned} \tag{8}$$

$$\begin{aligned}\delta_3 &= S_3 - S_0 + \delta_0 \\ &= \sqrt{\left(S_0\sin\beta_0 - V - \theta L_x\right)^2 + \left(S_0\cos\beta_0 - H\right)^2} - S_0 + \delta_0\end{aligned} \tag{9}$$

$$\begin{aligned}\delta_4 &= S_4 - S_0 + \delta_0 \\ &= \sqrt{\left(S_0\sin\beta_0 - V + \theta L_x\right)^2 + \left(S_0\cos\beta_0 + H\right)^2} - S_0 + \delta_0 .\end{aligned} \tag{10}$$

And the contact angle is shown as follows:

$$\begin{aligned}\sin\beta_1 &= \frac{S_0\sin\beta_0 + V - \theta L_x}{S_1} \\ &= \frac{S_0\sin\beta_0 + V - \theta L_x}{\sqrt{\left(S_0\sin\beta_0 + V - \theta L_x\right)^2 + \left(S_0\cos\beta_0 + H\right)^2}}\end{aligned} \tag{11}$$

$$\begin{aligned}\sin\beta_2 &= \frac{S_0\sin\beta_0 + V + \theta L_x}{S_2} \\ &= \frac{S_0\sin\beta_0 + V + \theta L_x}{\sqrt{\left(S_0\sin\beta_0 + V + \theta L_x\right)^2 + \left(S_0\cos\beta_0 - H\right)^2}}\end{aligned} \tag{12}$$

$$\begin{aligned}\sin\beta_3 &= \frac{S_0\sin\beta_0 - V - \theta L_x}{S_3} \\ &= \frac{S_0\sin\beta_0 - V - \theta L_x}{\sqrt{\left(S_0\sin\beta_0 - V - \theta L_x\right)^2 + \left(S_0\cos\beta_0 - H\right)^2}}\end{aligned} \tag{13}$$

$$\begin{aligned}\sin\beta_4 &= \frac{S_0\sin\beta_0 - V + \theta L_x}{S_4} \\ &= \frac{S_0\sin\beta_0 - V + \theta L_x}{\sqrt{\left(S_0\sin\beta_0 - V + \theta L_x\right)^2 + \left(S_0\cos\beta_0 + H\right)^2}} .\end{aligned} \tag{14}$$

Submitting Eqs. (7)-(10) to Eq. (3), the contact forces is obtained:

$$Q_1 = \xi(\delta_1)^{\frac{3}{2}} = \xi\left[\sqrt{(S_0\sin\beta_0 + V - \theta L_x)^2 + (S_0\cos\beta_0 + H)^2} - S_0 + \delta_0\right]^{\frac{3}{2}} \tag{15}$$

$$Q_2 = \xi(\delta_2)^{\frac{3}{2}} = \xi\left[\sqrt{(S_0\sin\beta_0 + V + \theta L_x)^2 + (S_0\cos\beta_0 - H)^2} - S_0 + \delta_0\right]^{\frac{3}{2}} \tag{16}$$

$$Q_3 = \xi(\delta_3)^{\frac{3}{2}} = \xi\left[\sqrt{(S_0\sin\beta_0 - V - \theta L_x)^2 + (S_0\cos\beta_0 - H)^2} - S_0 + \delta_0\right]^{\frac{3}{2}} \tag{17}$$

$$Q_4 = \xi(\delta_4)^{\frac{3}{2}} = \xi\left[\sqrt{(S_0\sin\beta_0 - V + \theta L_x)^2 + (S_0\cos\beta_0 + H)^2} - S_0 + \delta_0\right]^{\frac{3}{2}}. \tag{18}$$

According to Eqs. (15)-(18), the contact force is a function of V, H and θ. With the displacement increasing, the rolling balls may lose contact with the groove, the contact force Q_i will gradually decrease to zero, so Q_i is a piecewise nonlinear function of H, V and θ [14, 26]. The force acting on the carriage by the inside of rolling linear guide can be simplified as:

$$F_H = n(Q_1\cos\beta_1 - Q_2\cos\beta_2 - Q_3\cos\beta_3 + Q_4\cos\beta_4) \tag{19}$$

$$F_V = n(Q_1\sin\beta_1 + Q_2\sin\beta_2 - Q_3\sin\beta_3 - Q_4\sin\beta_4) \tag{20}$$

$$M_\theta = n((-Q_1\sin\beta_1 + Q_2\sin\beta_2 - Q_3\sin\beta_3 + Q_4\sin\beta_4)L_x + (Q_1\cos\beta_1 - Q_2\cos\beta_2 + Q_3\cos\beta_3 - Q_4\cos\beta_4)L_y) \tag{21}$$

where n is the number of rolling balls in each row; F_H, F_V and M_θ are horizontal force, vertical force and moment to the carriage, respectively.

2.4 Dynamic equations of motion of rolling linear guide

The load on rolling linear guide is harmonic excitation $\boldsymbol{F}$, and $\boldsymbol{F} = \overline{\boldsymbol{F}} + \overline{\boldsymbol{F}}_0\sin\varpi t$. Then, the horizontal load is $F_x = \overline{F}_x + \overline{F}_{x0}\sin\varpi t$; vertical load is $F_y = \overline{F}_y + \overline{F}_{y0}\sin\varpi t$; moment load is $M_Z = \left(\overline{F}_x + \overline{F}_{x0}\sin\varpi t\right)L_0$. As shown in Fig. 6, a three-DOF spring-mass vibration model of rolling linear guide system is established; k_H, c_H and k_V, c_V represent the equivalent stiffness and damping in the horizontal and vertical direction, respectively; I and k_θ are the moment of inertia and the equivalent rotational stiffness, respectively. ΔC_H and ΔC_V are the travel parallelism errors in the horizontal and vertical direction, respectively. Since the damping of rolling linear guide is mainly produced by the lubricating medium between the contact interfaces. Consequently, it is assumed that the relationship between the velocity and damping force is approximately linear [32].

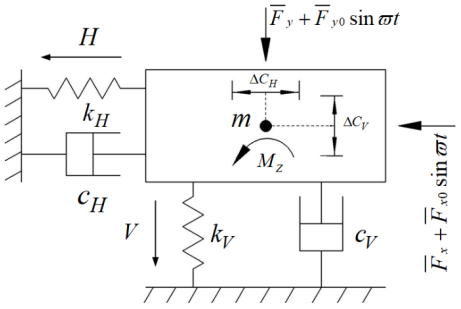

Fig. 6. Walking parallelism error of rolling linear guide in simplified three-DOF model.

From the above analysis, the dynamic motion equation of carriage is:

$$\begin{cases} m\ddot{H} + c_H\dot{H} + k_H H = \overline{F}_x + \overline{F}_{x0}\sin\varpi t \\ m\ddot{V} + c_V\dot{V} + k_V V = \overline{F}_y + \overline{F}_{y0}\sin\varpi t \\ I\ddot{\theta} + c_V\dot{\theta}L_x^2 + k_\theta\theta = M_Z. \end{cases} \tag{22}$$

According to analysis the load and contact deformation in Sec. 2, the contact stiffness coefficient of rolling balls and carriage k_i is a nonlinear function of the elastic deformation δ_i [7, 14]. According to the Eqs. (7)-(10), elastic deformation δ_i is a function of H, V and θ, so k_i is also a function of H, V and θ. In Eq. (22), $k_H H$, $k_V V$ and $k_\theta\theta$ represent the contact load of carriage caused by H, V and θ, respectively. However, k_H, k_V and k_θ are piecewise nonlinear function of H, V and θ [33]. In order to simplify the calculation process, $k_H H$, $k_V V$ and $k_\theta\theta$ are represented by forces that acting on carriage by inside of rolling linear guide, respectively [26]. From Eq. (9), the expression is as follows:

$$\begin{cases} k_H H = F_H(H,V,\theta) \\ k_V V = F_V(H,V,\theta) \\ k_\theta\theta = M_\theta(H,V,\theta). \end{cases} \tag{23}$$

Submitting Eq. (23) to Eq. (22), the dynamic motion equation of carriage system is obtained:

$$\begin{cases} m\ddot{H} + c_H\dot{H} + F_H(H,V,\theta) = \overline{F}_x + \overline{F}_{x0}\sin\varpi t \\ m\ddot{V} + c_V\dot{V} + F_V(H,V,\theta) = \overline{F}_y + \overline{F}_{y0}\sin\varpi t \\ I\ddot{\theta} + c_V\dot{\theta}L_x^2 + M_\theta(H,V,\theta) = M_Z. \end{cases} \tag{24}$$

When rolling linear guide bears the vertical load F_y, the above method can be used to establish a single degree of freedom dynamic motion equation. If rolling linear guide is sub-

jected to load F_x and F_y, the dynamic equation of two-DOF can be obtained in the same way.

It can be seen from Eq. (24) that the dynamic equation of rolling linear guide is relatively complex, and the parameters are coupled with each other. Accordingly, it is difficult to obtain the analytical solution. Therefore, the four-order-Runge-Kutta method is used to solve the problem, and the dynamic response value of rolling linear guide at each moment is obtained.

3. Dynamic reliability analysis of rolling linear guide

3.1 Interval model of geometric parameters

Interval number D^I refers to any pair of closed bounded real numbers [34]:

$$D^I=\left[D^L,D^U\right]=\left\{D\mid D^L\le D\le D^U\right\} \tag{25}$$

where the superscripts L and U represent the lower and upper limit of interval number, respectively.

The midpoint(D^c) and radius(D^w) of the interval number are expressed as:

$$\begin{cases} D^c=\dfrac{D^L+D^U}{2} \\ D^w=\dfrac{D^U-D^L}{2}. \end{cases} \tag{26}$$

Therefore, the interval number can also be expressed as:

$$D^I=D^c+\left[-1,1\right]D^w. \tag{27}$$

The dynamic performance of rolling linear guide is affected by several geometric parameters, including initial contact angle β_0, rolling ball diameter d_0, groove curvature r_c and initial deformation δ_0 [14]. Due to the existence of dimensional tolerance of the parts and the influence of random factors in the manufacturing and assembly process, geometric parameters are uncertain. Hence, interval model is used to express the uncertainty of the geometric parameters. Supposing the uncertainty of geometric parameters is η, the value range of the above geometric parameters is:

$$\begin{cases} \beta_0^I=\left[\overline{\beta_0}-\eta\overline{\beta_0},\ \overline{\beta_0}+\eta\overline{\beta_0}\right] \\ d_0^I=\left[\overline{d_0}-\eta\overline{d_0},\overline{d_0}+\eta\ \overline{d_0}\right] \\ r_c^I=\left[\overline{r_c}-\eta\,\overline{r_c},\ \overline{r_c}+\eta\ \overline{r_c}\right] \\ \delta_0^I=\left[\overline{\delta_0}-\eta\,\overline{\delta_0},\ \overline{\delta_0}+\eta\,\overline{\delta_0}\right] \end{cases} \tag{28}$$

where β_0^I, d_0^I, r_c^I and δ_0^I are interval values of geometric parameters, respectively; $\overline{\beta_0}$, $\overline{d_0}$, $\overline{r_c}$ and $\overline{\delta_0}$ are the design values.

3.2 Reliability analysis based on interval model

The dynamic performance of rolling linear guide is represented by the walking parallelism error ΔC, it can be determined according to the specification and grade of rolling linear guide. If the parallelism tolerance threshold ΔC is determined, the reliable range of the dynamic motion of carriage at time t is $E(t)^I$:

$$E(t)^I=\left[E(t)^L,E(t)^U\right]=\left[\overline{T}(t)-\frac{1}{2}\Delta C,\overline{T}(t)+\frac{1}{2}\Delta C\right]. \tag{29}$$

$\overline{T}(t)$ and $T(t)$ represent the expected displacement and the actual displacement, respectively. Thus, the dynamic reliability of rolling linear guide at time t can be computed as:

$$R(t)=P\left(E(t)^L\le T(t)\le E(t)^U\right). \tag{30}$$

The vector ϕ indicates the set of geometric parameters, $\phi=\left\{\beta_0^I,d_0^I,r_c^I,\delta_0^I\right\}$. The displacement of carriage is a nonlinear function of geometric parameters. Therefore, the state function $g(\phi,t)$ is introduced, and its response value at time t represents the displacement value of carriage, i.e., $T(t)=g(\phi,t)$.

The state function $g(\bullet)$ is a continuous function of vector ϕ and therefore the displacement response value at time t is also an interval variable [35, 36], i.e., $T(t)=\left[T(t)^L,T(t)^U\right]$.

As shown in Fig. 7, there are many position relations between the displacement range and the reliable range of carriage. The dynamic reliability $R(t)$ of rolling linear guide at time t can be computed as:

$$R(t)=\begin{cases} 0, & T(t)^U\le E(t)^L \\ & T(t)^L\ge E(t)^U \end{cases} \text{ or}$$
$$\begin{cases} \dfrac{T(t)^U-E(t)^L}{T(t)^U-T(t)^L}, & T(t)^L<E(t)^L \\ & E(t)^L<T(t)^U<E(t)^U \end{cases} \text{ and}$$
$$\begin{cases} \dfrac{E(t)^U-T(t)^L}{T(t)^U-T(t)^L}, & T(t)^U>E(t)^U \\ & E(t)^L<T(t)^L<E(t)^L \end{cases} \text{ and}$$
$$\begin{cases} \dfrac{E(t)^U-E(t)^L}{T(t)^U-T(t)^L}, & T(t)^L<E(t)^L \\ & T(t)^U>E(t)^U \end{cases} \text{ and}$$
$$\begin{cases} 1, & T(t)^L\ge E(t)^L \\ & T(t)^U\le E(t)^U. \end{cases} \text{ and} \tag{31}$$

The nonlinear relationship between state function $g(\bullet)$ and geometric parameters. Hence it is difficult to accurately solve the displacement interval value. Therefore, the genetic algorithm is combined with the dynamic equations of motion to solve the displacement boundary [24]. By comparing the posi-

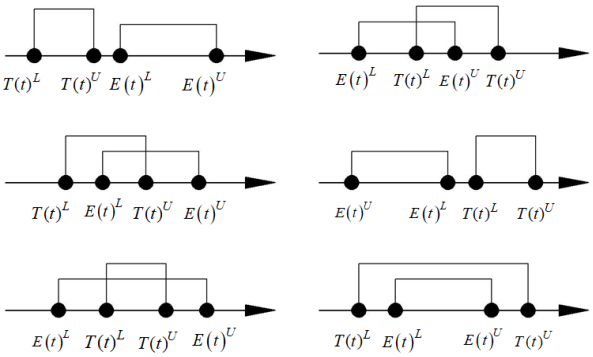

Fig. 7. Position relationship between displacement interval and reliable interval.

tion relationship between the displacement interval and the reliable interval, the dynamic reliability of rolling linear guide is calculated by Eq. (31).

On the basis of analysis in Sec. 2, the rolling linear guide subject to the load of F_x, F_y and M_Z. The carriage has vertical displacement V and horizontal displacement H. The above method is used to calculate the vertical dynamic reliability $R_V(t)$ and horizontal dynamic reliability $R_H(t)$ at time t.

Finally, the comprehensive dynamic reliability $R(t)$ at time t is:

$$R(t) = \min\left(R_V(t), R_H(t)\right). \tag{32}$$

3.3 Dynamic reliability calculation program

As shown in Fig. 8, the dynamic performance reliability analysis process is as follows:

Step 1: Establishing the force model of rolling linear guide, and analyze the load and contact deformation;

Step 2: A three-DOF dynamic motion model of carriage is established;

Step 3: Determining the parallelism tolerance threshold, and solving the dynamic equation of model to obtain the ideal values of vertical displacement V and horizontal displacement H of carriage at time t. Using the Eq. (29), the dynamic reliable intervals of the vertical and horizontal direction of carriage are obtained;

Step 4: The interval value of geometric parameters is calculated by Eq. (28). Then, combining genetic algorithm, the boundary of the dynamic response interval value of carriage in two directions at time t are solved;

Step 5: Using the reliability calculation method of Eq. (31), the dynamic reliability of vertical and horizontal direction at time t are obtained;

Step 6: The comprehensive dynamic reliability at time t is obtained by the calculation method of Eq. (32);

Step 7: If the cut-off time t_{end} is reached, ended the calculation and output the result; Otherwise, return to step 3 to calculate the dynamic reliability at the next moment.

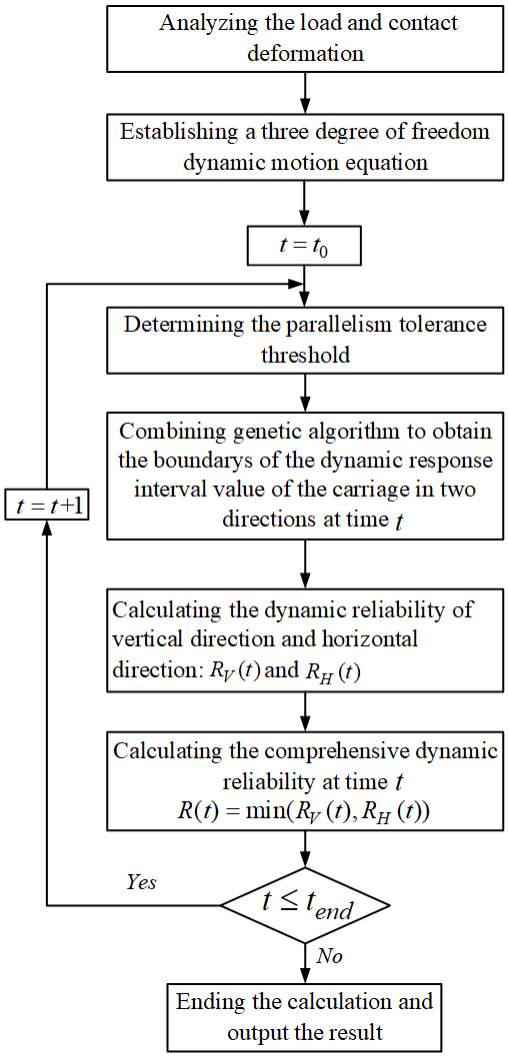

Fig. 8. Flow chart of dynamic reliability analysis.

4. Numerical example

4.1 Rolling linear guide model

The dynamic reliability of SHS-45R rolling linear guide is analyzed by using the proposed method in this paper, and the parameters are illustrated in Table 1. The excitation force $\bar{F}$ is 15000 N and the mean force $\bar{F}_0$ is 10000 N, the excitation frequency is 5π. The angle between working load and vertical direction is 30° ($\alpha = 30°$).

4.2 Dynamic response analysis

When the geometric parameters are ideal, the single-DOF dynamic response of rolling linear guide is calculated by using the load conditions in Ref. [14]. The comparison results of the dynamic response values of rolling linear guide calculated by the model in this paper with the Ref. [14] is shown in Fig. 9. It can be concluded that under the same load conditions, the vertical dynamic response results of the rolling linear guide are

Table 1. Specifications of rolling linear guide.

Number of race ways	4	Initial deformation of ball	3.6 μm
Number of the loaded balls in a raceway	10	Initial contact angle	45°
Diameter of the ball	6.53 mm	L_x	20 mm
Radii of the groove	3.5 mm	L_y	9 mm
Poisson's ratio: $\boldsymbol{v}_1$ $\boldsymbol{v}_2$	0.3	L_0	38 mm
Elasticity modulus: $\boldsymbol{E}_1$ $\boldsymbol{E}_2$	206 GPa	Mass	3.24 kg

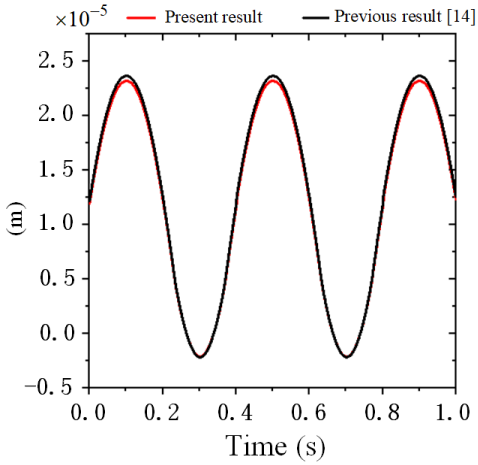

Fig. 9. Comparative analysis of dynamic model analysis results.

basically consistent. Therefore, the calculation accuracy of the dynamic analysis model established in this paper meets the analysis requirements.

Then, the dynamic characteristics of rolling linear guide is analyzed by using two-DOF dynamic motion model and three-DOF dynamic motion model. As shown in Fig 10, the dynamic response of vertical displacement and horizontal displacement are obtained. Figs. 10(a) and (b) are the dynamic response of two-DOF motion model and three-DOF motion model, respectively.

It can be seen from Fig. 10(a), the rolling linear guide is only loaded F_x and F_y. Since the load F_y is greater than F_x, the vertical displacement V is always greater than the horizontal displacement H in the same moment. However, as shown in Fig. 10(b), the rolling linear guide is loaded F_x, F_y and M_Z.The vertical displacement response V is less than horizontal displacement response H in the same moment. Moreover, the displacement dynamic response value calculated by three-DOF motion model is far greater than that calculated by two-DOF motion model. The main reason for this phenomenon is that the load M_Z changes the contact state between rolling balls and groove, and the dynamic contact stiffness is changed. Next, the contact angle and equivalent stiffness of the two dynamic models are analyzed.

The equivalent dynamic stiffness in horizontal and vertical directions of rolling linear guide that calculated by two-DOF motion model and three-DOF motion model is illustrated in Fig. 11. The equivalent stiffness of the two directions of the two-DOF motion model is greater than that of the three-DOF motion model. Therefore, due to the decrease of equivalent stiffness, the horizontal displacement and vertical displacement in the three-DOF motion model are larger.

In the three-DOF motion model, the contact angle between rolling balls and groove changes due to the action of load M_Z, resulting in the decrease of equivalent stiffness coefficient in horizontal and vertical directions. Fig. 12 shows the change of the contact angle, Figs. 12(a) and (b) are the results that calculated by two-DOF motion model and three-DOF motion model respectively. Fig. 13 shows the dynamic response of deflection angle θ in the three-DOF motion model. Because of the deflection angle θ, the change range of contact angle in two-DOF motion model is smaller than that of three-DOF motion model. As shown in Fig. 12(b), in horizontal direction, due to the contact angle β_4 increases, the load is mainly borne by the $1\text{-}th$ row of rolling balls, so the horizontal displacement increases and the contact stiffness coefficient decreases. In the vertical direction, the load is originally borne by the $1\text{-}th$ and $2\text{-}th$ row of rolling balls. Due to the decrease of β_1 and the increase of β_2, the load on the $2\text{-}th$ row of rolling balls decreases, and the load on the $1\text{-}th$ row of rolling balls increases, so the vertical displacement increases, and the equivalent stiffness decreases. Accordingly, the horizontal displacement value is greater than the vertical displacement value, as shown in Fig. 10(b).

It can be seen from Figs. 10 and 11 that the displacement response is inversely proportional to the equivalent stiffness in the two-DOF motion model. And in the three-DOF motion model, the displacement response is proportional to the equivalent stiffness. That is because the relationship between stiffness coefficient and displacement of linear rolling guide is nonlinear. With the increase of displacement, the stiffness coefficient decreases gradually. When the displacement reaches the threshold value, the stiffness coefficient is the minimum. Then, the displacement continues to increase, and the stiffness coefficient increases linearly with the displacement [8, 14, 26].

So, in the two-DOF motion model, the load is borne by two rows of balls, and the displacement response value is less than the threshold value, and the displacement response is inversely proportional to the equivalent stiffness. In the three-DOF motion model, due to the deflection angle θ, the load is mainly concentrated in one row of balls, which makes the dis-

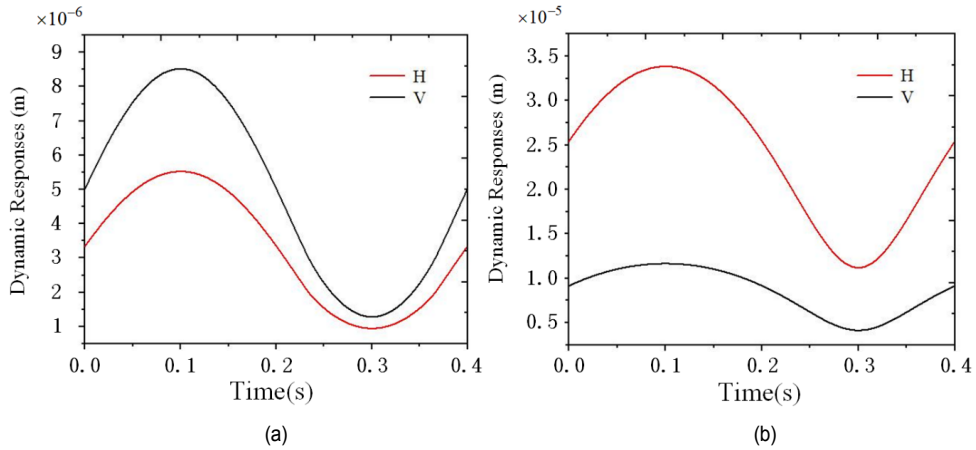

Fig. 10. Horizontal displacement H and vertical displacement V: (a) dynamic response of two-DOF; (b) dynamic response of three-DOF.

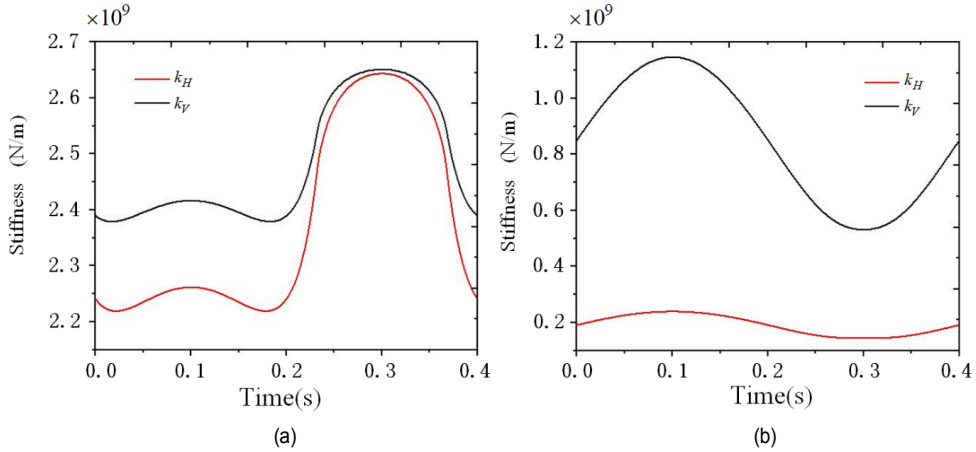

Fig. 11. Equivalent stiffness in vertical and horizontal direction: (a) analysis results of two-DOF model; (b) analysis results of three-DOF model.

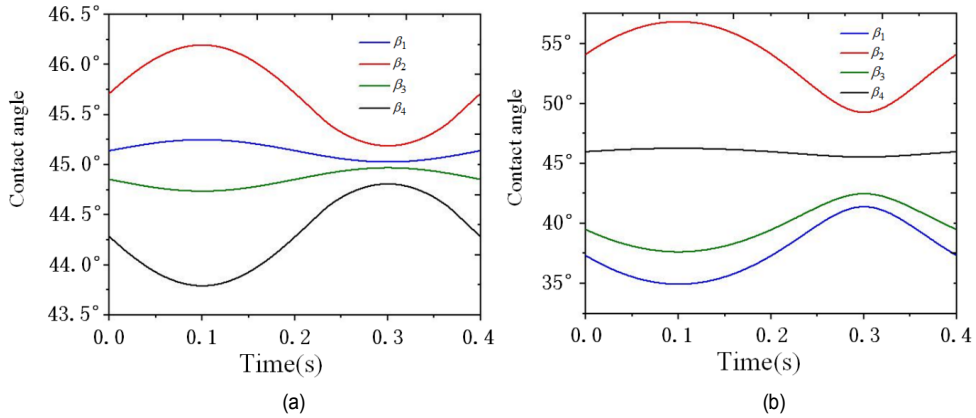

Fig. 12. Changing of the contact angle: (a) analysis results of two-DOF model; (b) analysis results of three-DOF model.

placement response value greater than the threshold value, and the displacement response is proportional to the equivalent stiff ness.

According to the above analysis, the load M_z plays crucial role in the dynamic characteristics of rolling linear guide. Considering the complexity of the load in the actual project, the three-DOF dynamic motion model is established, so the dynamic reliability is evaluated accurately.

4.3 Reliability evaluation

In this section, the dynamic reliability of SHS-45R is evalu-

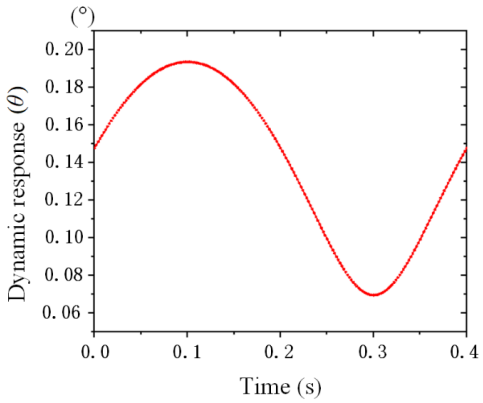

Fig. 13. Dynamic response of deflection angle.

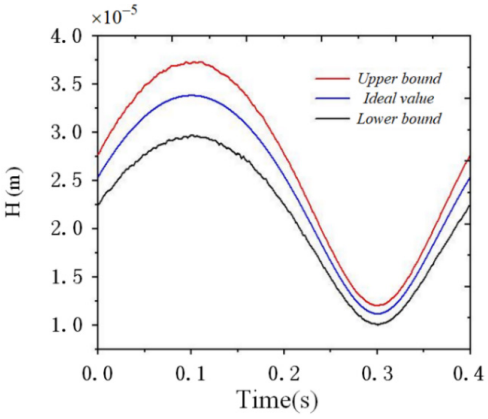

(a)

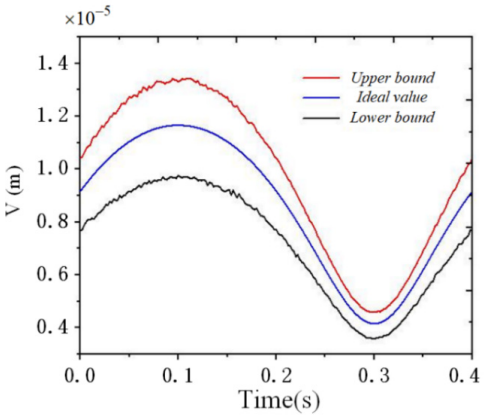

(b)

Fig. 14. Dynamic displacement response under uncertainty: (a) dynamic response of horizontal displacement (H); (b) dynamic response of vertical displacement (V).

ated by using three-DOF dynamic motion model. The walking parallelism tolerance of a high precision rolling linear guide is 3 μm . Hence the reliable range of the dynamic motion of carriage is obtained by Eq. (29). Suppose the uncertainty of geometric parameters $\left[\beta_0, d_0, r_c, \delta_0\right]$ is: $\eta = 0.02$. Therefore, the interval value of geometric parameters can be obtained from

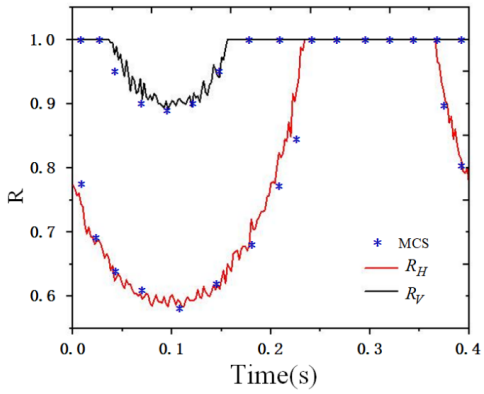

Fig. 15. Dynamic reliability of horizontal and vertical direction.

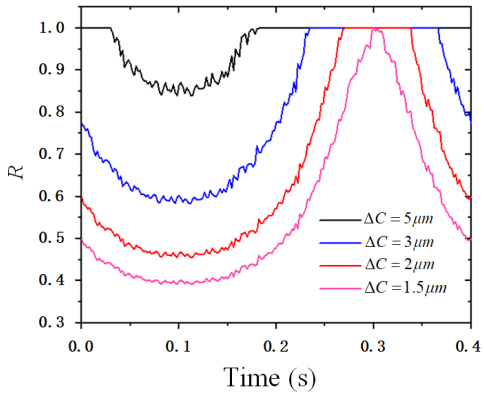

Fig. 16. Comprehensive dynamic reliability of different accuracy grades.

Eq. (28).

The distribution of the maximum, minimum and ideal values of horizontal and vertical displacement dynamic response under uncertainty are shown in Fig. 14. Where, Figs. 14(a) and (b) represent horizontal displacement and vertical displacement respectively. In each moment, the maximum and minimum displacement are located on both sides of the ideal value, so the displacement is interval value.

Using the interval reliability calculation method described in Sec. 3, the dynamic reliability of horizontal and vertical direction is analyzed, and the dynamic reliability is shown in Fig. 15. In order to verify the effective of the method, the reliability of rolling linear guide is also evaluated by Monte Carlo simulation (MCS) method. Through comparative analysis of calculation results, the error is less than 5 %, which shows that the calculation accuracy of the method is high.

Although the vertical load of rolling linear guide is greater than the horizontal load, the load M_Z changes the contact state between rolling balls and groove. Consequently, the equivalent stiffness in horizontal direction is smaller than that in vertical direction. Considering the uncertainty of parameters, the horizontal displacement fluctuates greatly, and the dynamic reliability of rolling linear guide changes greatly and the reliability is low. However, the vertical displacement fluctuation is

small, so the dynamic reliability change in vertical direction is small and the reliability is high. Moreover, the dynamic reliability in vertical direction is higher than that in horizontal direction. According to Eq. (32), the comprehensive dynamic reliability is the horizontal dynamic reliability, i.e., $R(t) = R_H(t)$.

According to the different motion accuracy grades, the rolling linear guide can be divided into ordinary grade, high grade, precision grade and super precision grade. And the corresponding walking parallelism tolerances is $5\ \mu m$, $3\ \mu m$, $2\ \mu m$ and $1.5\ \mu m$, respectively. The dynamic reliability of rolling linear guide is evaluated by the method described in this paper. The comprehensive dynamic reliability is shown in Fig. 16. Under the same load, with increasing accuracy grade of rolling linear guide, the allowable walking parallelism tolerance gradually decreases, and the comprehensive dynamic reliability decreases gradually.

5. Conclusions

This paper presents a dynamic reliability analysis method of rolling linear guide considering the uncertainty of geometric parameters. The reliability range of dynamic response is determined according to the accuracy grade of rolling linear guide. A dynamic motion model considering the contact characteristics is established by using the Hertz contact theory.

By comparing the analysis results of two-DOF dynamic motion model and three-DOF dynamic motion model, the load M_Z plays crucial role in the dynamic characteristics of rolling linear guide. Therefore, considering the complexity of the load in the actual project, the dynamic characteristics is analyzed by using the three-DOF motion model.

In order to improve the accuracy of reliability evaluation, interval model is used to express the uncertainty of geometric parameters. As a result, the horizontal and vertical dynamic displacement responses of rolling linear guide are also interval numbers. The interval reliability calculation method is used to analyze and calculate the horizontal and vertical dynamic reliability.

The dynamic reliability of SHS-45R is analyzed by using the reliability evaluation method described in this paper, and at the same time, the dynamic reliability is evaluated by Monte Carlo simulation. The calculation results show that the proposed method is effective. And the computation error is less than 5 %. The comprehensive dynamic reliability of rolling linear guide with different accuracy grades is evaluated. With increasing accuracy grade, the allowable walking parallelism tolerance gradually decreases, and the dynamic reliability of rolling linear guide decreases gradually. It provides a new method for dynamic reliability evaluation of rolling linear guide in practical application.

Acknowledgments

This work was supported by the National Natural Science Foundation of China [Grant numbers 51705048 and 51835001].

References

[1] P. Albertelli, N. Cau, G. Bianchi and M. Monno, The effects of dynamic interaction between machine tool subsystems on cutting process stability, *The International Journal of Advanced Manufacturing Technology*, 58 (9-12) (2012) 923-932.

[2] C. Y. Lin, J. P. Hung and T. L. Luo, Effect of preload of linear guides on dynamic characteristics of a vertical column-spindle system, *International Journal of Machine Tools and Manufacture*, 50 (8) (2010) 741-746.

[3] J. P. Hung, Y. L. Lai, C. Y. Lin and T. Z. Luo, Modeling the machining stability of a vertical milling machine under the influence of the preloaded linear guide, *International Journal of Machine Tools and Manufacture*, 51 (9) (2011) 731-739.

[4] Y. S. Yi, Y. Y. Kim, J. S. Choi, J. Yoo, D. J. Lee, S. W. Lee and S. J. Lee, Dynamic analysis of a linear motion rolling guide having rolling elements for precision positioning devices, *Journal of Mechanical Science and Technology*, 22 (1) (2008) 50-60.

[5] H. T. Zou and B. L. Wang, Investigation of the contact stiffness variation of linear rolling guides due to the effects of friction and wear during operation, *Tribology International*, 92 (2015) 472-484.

[6] W. Tao, Y. Zhong, H. Feng and Y. Wang, Model for wear prediction of roller linear guides, *Wear*, 305 (1-2) (2013) 260-266.

[7] X. P. Li, Y. M. Liang, H. T. Yang, X. Ju and G. H. Zhao, Influence of bolt joint on dynamic characteristic of linear rolling guide, *Applied Mechanics and Materials,* 307 (2013) 182-185.

[8] X. X. Kong, W. Sun, B. Wang and B. C. Wen, Dynamic and stability analysis of the linear guide with time-varying, piecewise-nonlinear stiffness by multi-term incremental harmonic balance method, *Journal of Sound and Vibration*, 346 (1) (2015) 265-283.

[9] V. C. Tong, G. Khim, S. W. Hong and C. H. Park, Construction and validation of a theoretical model of the stiffness matrix of a linear ball rolling guide with consideration of carriage flexibility, *Mechanism and Machine Theory*, 140 (2019) 123-143.

[10] G. I. Schuëller and H. A. Jensen, Computational methods in optimization considering uncertainties - an overview, *Computer Methods in Applied Mechanics and Engineering*, 198 (1) (2008) 2-13.

[11] S. S. Rao and P. K. Bhatti, Probabilistic approach to manipulator kinematics and dynamics, *Reliability Engineering and System Safety*, 72 (1) (2001) 47-58.

[12] C. Li, W. Wang, Y. Zhang, S. Guo, Z. Li and C. Qiao, Indexing accuracy reliability sensitivity analysis of power tool turret, *Eksploatacja i Niezawodnosc-Maintenance and Reliability*, 17 (1) (2015) 27-34.

[13] D. Zhou, X. Zhang and Y. Zhang, Dynamic reliability analysis for planetary gear system in shearer mechanisms, *Mechanism and Machine Theory*, 105 (2016) 244-259.

[14] W. Wang, Y. M. Zhang and C. Y. Li, Dynamic reliability analysis of linear guides in positioning precision, *Mechanism and Machine Theory*, 116 (2017) 451-464.

[15] S. Q. Qiu and H. X. G. Ming, Reliability analysis of multi-state

series systems with performance sharing mechanism under epistemic uncertainty, *Quality and Reliability Engineering International*, 35 (7) (2019) 1998-2015.
[16] R. X. Wang, X. Gao, Z. Y. Gao, S. Q. Li, J. M. Gao, J. J. Xu and W. Deng, Comprehensive reliability evaluation of multi-state complex electromechanical systems based on similarity of cloud models, *Quality and Reliability Engineering International*, 36 (3) (2020) 1048-1073.
[17] B. Möller and M. Beer, Engineering computation under uncertainty-capabilities of non-traditional models, *Computers & Structures*, 86 (10) (2008) 1024-1041.
[18] L. Zhang, J. G. Zhang, L. F. You and S. Zhou, Reliability analysis of structures based on a probability-uncertainty hybrid model, *Quality and Reliability Engineering International*, 35 (4) (2019) 263-279.
[19] Y. Ben-Haim, *Convex Models of Uncertainty in Applied Mechanics*, Elsevier Science Publishers, New York, USA (1990) 151-157.
[20] J. Cheng, M. Y. Tang, Z. Y. Liu and J. R. Tan, Direct reliability-based design optimization of uncertain structures with interval parameters, *Journal of Zhejiang University-Science A: Applied Physics & Engineering*, 17 (11) (2016) 841-854.
[21] Z. Qiu, Comparison of static response of structures using convex models and interval analysis method, *International Journal for Numerical Methods in Engineering*, 56 (12) (2003) 1735-1753.
[22] C. Jiang, X. Han and G. R. Liu, Optimization of structures with uncertain constraints based on convex model and satisfaction degree of interval, *Computer Methods in Applied Mechanics and Engineering*, 196 (49) (2007) 4791-4800.
[23] J. L. Wu, Z. Luo, N. Zhang and Y. Q. Zhang, A new interval uncertain optimization method for structures using Chebyshev surrogate models, *Computers & Structures*, 146 (2015) 185-196.
[24] J. Cheng, Z. Y. Liu, M. Y. Tang and J. R. Tan, Robust optimization of uncertain structures based on normalized violation degree of interval constraint, *Computers & Structures*, 182 (2017) 41-54.
[25] X. G. Yu, X. Wang, X. T. Liu and Y. S. Wang, Reliability reallocation for cost uncertainty of fuel cell vehicles via improved differential evolution algorithm, *Quality and Reliability Engineering International*, 36 (2020) 303-314.
[26] W. Wang, C. Y. Li, Y. X. Zhou, H. Wang and Y. M. Zhang, Nonlinear dynamic analysis for machine tool table system mounted on linear guides, *Nonlinear Dynamics*, 94 (7) (2018) 2033-2045.
[27] Z. T. Fu, X. M. Zhang, X. L. Wang and W. Y. Yang, Analytical modeling of chatter vibration in orthogonal cutting using a predictive force model, *International Journal of Mechanical Sciences*, 88 (6) (2014) 145-153.
[28] B. Li, X. Wang, Y. Hu and C. Li, Analytical prediction of cutting forces in orthogonal cutting using unequal division shear-zone model, *The International Journal of Advanced Manufacturing Technology*, 54 (5-8) (2011) 431-443.
[29] J. Gu, J. S. Agapiou and S. Kurgin, CNC machine tool work offset error compensation method, *Journal of Manufacturing Systems*, 37 (2015) 576-585.
[30] H. Ohta and K. Tanaka, Vertical stiffnesses of preloaded linear guideway type ball bearings incorporating the flexibility of the carriage and rail, *Journal of Tribology*, 132 (1) (2010) 547-548.
[31] T. Harris, *Rolling Bearing Analysis,* Wiley, New York, USA (1991).
[32] L. Bizarre, F. Nonato and K. L. Cavalca, Formulation of five degrees of freedom ball bearing model accounting for the nonlinear stiffness and damping of elastohydrodynamic point contacts, *Mechanism and Machine Theory*, 124 (2018) 179-196.
[33] W. Wang, Y. M. Zhang, C. Y. Li, H. Wang and Y. X. Zhou, Effects of wear on dynamic characteristics and stability of linear guides, *Meccanica*, 52 (111-12) (2017) 2899-2913.
[34] R. E. Moore, *Methods and Applications of Interval Analysis,* SIAM, Philadelphia, USA (1979).
[35] Z. P. Qiu and L. Wang, The need for introduction of non-probabilistic interval conceptions into structural analysis and design, *Science China Physics, Mechanics & Astronomy*, 59 (11) (2016) 90-92.
[36] C. M. Fu, Y. X. Liu and Z. Xiao, Interval differential evolution with dimension-reduction interval analysis method for uncertain optimization problems, *Applied Mathematical Modelling*, 69 (2019) 441-452.

Li Jian is currently pursuing the Ph.D. degree in Mechanical Engineering with Chongqing University. His research interests include reliability technology, failure analysis of CNC machine tool, and advanced manufacturing technology.

Ran Yan is currently a lecturer at Chongqing University, a fixed researcher at the State Key Laboratory of Mechanical Transmission, Chongqing University, a member of the Chongqing Science and Technology Association and a member of the National Association of Basic Research on Interchangeability and Measurement Technology. Her research interests include mechatronic product reliability technology and modern quality engineering.